Kufa Journal of Engineering
Vol. 7, No. 2, June 2016, P.P. 20-37
Received 24 August 2015, accepted 10 February 2016

THERMAL LOSSES REDUCTION FOR A TROUGH SOLAR COLLECTOR: PART 1 FLUID FLOW

Wisam A. Abd Al-Wahid[1] and Dhafer M. H. Al-Shamkhee[2]

[1] Automotive Technical Engineering Dept, Technical Engineering College/Najaf, AL-Furat AL-Awsat Technical University, Email wsm19782000@gmail.com

[2] Alternative and Renewable Energy Research Unit, Technical Engineering College/Najaf, AL-Furat AL-Awsat Technical University, Email dhafeer_manee@yahoo.com

ABSTRACT

The flow of the wind near an absorber of a trough collector is analyzed. Since this absorber loss useful heat into the ambient, it is necessary to reduce that heat. The common strategy of reduction is the use of a vacuum tube. The maintaining of vacuum is difficult due to air leak or glass fracture led to find another replacement for this strategy. The idea of the present work is to put a half circular disc in front of the receiver in order to reduce the air velocity near the tube and reduce the heat transfer process. The flow is analyzed in the area to find the streamlines of flow and the behavior of air for a different air velocities and trough orientations. The analysis is done by using COMSOL Multiphysics program V4.4. The data show that the overall air velocity is reduced near the receiver as predicted.

KEYWORDS

Thermal losses reduction; Trough collector; solar energy.

تقليل الخسائر الحرارية من مجمع شمسي: الجزء الاول جريان المائع

وسام عبد الواحد وظافر الشمخي

الكلية التقنية الهندسية/ جامعة الفرات الاوسط

الخلاصة

في هذا البحث، تم تحليل جريان الرياح بالقرب من انبوب التجميع في المجمع الشمسي. وقد وجد بأن الالية المتبعة لتقليل انتقال الحرارة هي باستخدام انبوب مفرغ من الهواء يغطي انبوب التجميع. وبما ان تكلفة هكذا انبوب هي عالية ناهيك عن صعوبة المحافظة على التفريغ بسبب التسرب أو كسر الانبوب. لذا فقد قدم هذا البحث اسلوب جديد في تقليل الخسائر يقضي بوضع مصدّات هوائية على شكل نصف دائري وبمختلف الاقطار أمام انبوب التجميع وذلك للتأثير في عملية انتقال الحرارة. حيث تم تحليل الجريان وأيجاد خطوط جريان الهواء عند سرع جريان مختلفة واتجاهات مختلفة للمجمع الشمسي. وقد تم استخدام برنامج COMSOL MULTIPHYSICS V4.4 لغرض التحليل الرياضي المتبع. اظهرت النتائج التي تم التوصل اليها ان سرعة الهواء قرب انبوب التجميع في المجمع الشمسي تقل كما متوقع.

NOMENCLATURES

Symbol	Description	Units
c_p	Thermal expansion coefficient	J/kg.K
D	Cylinder diameter	m
Dhi	Hydraulic diameter at interring	m
Dr	Diameter ratio	
F	Volume force	N/m^3
K	Thermal conductivity	W/m.K
k	Turbulent kinetic energy	m^2/s^2
L_T	Turbulence length scale	m
l_T	Turbulence intensity	m^2/s^2
Nu	Local Nusselt number	
Nua	Average Nusselt number	
Nu_{fsp}	Average Nusselt number at front	
Nu_{max}	Maximum Average Nusselt number	
Nu_{min}	Minimum Average Nusselt number	
p	Pressure	N/m^2
P_o	Outlet pressure	N/m^2
Pr	Prandtl number	
Re_i	Reynolds number at inlet	
T	Temperature	K
T_{amb}	Ambient Temperature	K
Trt	Receiver tube temperature	K
Ttw	Trough wall temperature	K
U	Velocity field (u,v,w)	m/s
u	Horizontal velocity	m/s
v	Vertical velocity	m/s
W	Aperture of the parabolic collector	m
x	Horizontal coordinate	m
y	Vertical coordinate	m

GREEK SYMBOLS

Symbol	Description	Units
ρ	Density of air	kg/m^3
μ	Dynamic viscosity	$N.s/m^2$
μ_T	Turbulent Dynamic viscosity	$N.s/m^2$
ε	Rate of dissipation of kinetic energy	m^2/s^2
θ	Pitch angle	degree

1. INTRODUCTION

Solar energy may transform indirectly into electric power by using the Solar Trough Collectors (STC) as the heat source in Rankine power stations (Naeeni, N, and Yaghoubi, M.,2007). (STC) is made by bending a sheet of reflective material to a parabolic shape, where this collector concentrates the solar energy over an absorber tube to transfer it to the working fluid flowing inside the tube (Padilla, Ricardo Vasquez, et. al, 2011). This process causes an increase in the absorber's temperature. The high temperature is useful for the process of energy production, so it is very important to conserve that heat. The reduction of the losses from the tube takes a great attention because of its importance. The absorber tube, may be covered by a vacuumed glass tube to reduce heat loss (Padilla, Ricardo Vasquez, et. al, 2011), and (Kalogirou, Soteris, 2012). Sometimes a certain composition of vacuumed glasses is used (Daniel, Premjit, et. al., 2011). It is true for the difficulty of keeping the vacuum inside the glass tube, but still the vacuum tube is the best strategy to reduce heat losses to the ambient. In the other hand some the difficulty and started a new strategy, such as the insulation of half the tube that is not facing the reflective collector (Al-Ansary, Hany, and Zeitoun, O., 2011).

The heat lost from the receiver into the ambient air passing over the (STC). It is found that the position of the trough to the blowing air affect the heat transfer process from the receiver to the ambient (Naeeni, N, and Yaghoubi, M., 2007), and (Naeeni, N, and Yaghoubi, M., 2007), which is because the effect on the flow near the receiver tube. Another effect of that wind to be found on the structure of the whole (STC) due to the lift and drag forces where the curvature of the trough has a great effect on that forces (Kazem, Aladine Abdulkader, and Hussein, Khalid Hameed, 2013). The studies of that kind may be depending on the general cases of air flowing over bodies (Gu, Ming, 2009). The importance of that study is due to the fact that, (STCs) are established in an open spaces which make them far from the boundary layer of the winds, which affect the stability of the trough during tracking the sun over the day (Cheng, Z. D., et.al., 2012). Studies may tabulate the lift and drag forces on the trough in order to take them in mind in the design (Gong, Bo, et.al, 2012).

It is found that the existence of trees or anybody on the track of the air toward the (STC) has a big effect on the lift and drag forces and finally heat transfer process (Christo, Farid C., 2012). The present work presents a new strategy to reduce the heat loss from the receiver tube by inserting a half-circular plate in front of the receiver. Three angles of collector's orientations values taken as shown in Fig.1. The effect of this plate on the fluid flow is studied in a turbulent two-dimensional domain as shown in Fig.2.

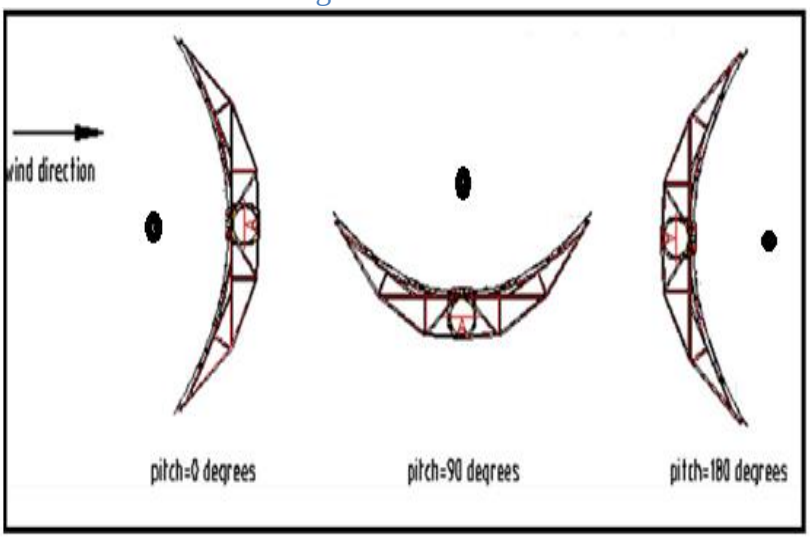

Fig. 1. The orientations of the present work

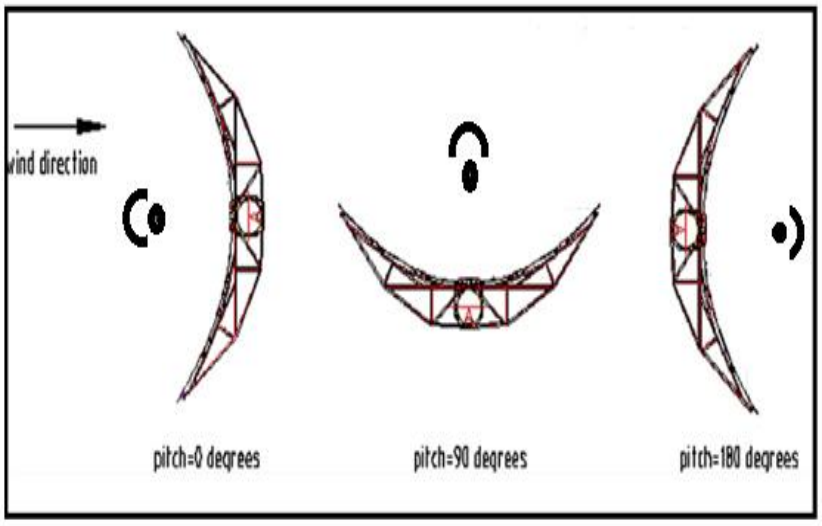

Fig. 2. The suggested modification in the present work

2. MATHEMATICAL MODEL

The velocity, temperature, and the streamlines of the domain obtained in order to find the effect of the addition of the circular plate.

The trough fixed with the ambient temperature, about 300 K. The absorber tube fixed in the middle of the trough with a temperature of 350 ^{o}K, and a diameter of 11.5 cm.

All the properties assumed constant, the flow is horizontal of 300 ^{o}K, and the absorber surface temperature is uniform at the whole surface. Since the aspect ratio between the troughs diameter to the receiver diameter is very big, then the problem assumed two-dimensional. Regarding combined free and force convection when the ratio of Gr/Red^2 =1, momentum equation is different and buoyancy should be included as described in (Hachicha, A. A., et.al, 2012).

The governing equations for 2-D steady state incompressible continuity equation is;

$$\nabla.(\rho U) = 0 \tag{1}$$

, the time averaged Navier-Stokes equations

$$\rho(U.\nabla)U = \nabla.\left[-PL + (\mu + \mu_T)(\nabla U + (\nabla U)^T) - \frac{2}{3}(\mu + \mu_T)(\nabla.U)l - \frac{2}{3}\rho k_l\right] + F \tag{2}$$

, the RNG-based k-ε turbulent scheme equations:

$$\rho(U.\nabla)k = \nabla.\left[\left(\mu + \frac{\mu_T}{\sigma_k}\right)\nabla k\right] + P_k - \rho\epsilon \tag{3}$$

$$\rho(U.\nabla)\epsilon = \nabla.\left[\left(\mu + \frac{\mu_T}{\sigma_e}\right)\nabla\epsilon\right] + C_{e1}\frac{\epsilon}{k}P_k - C_{e2}\rho\frac{\epsilon^2}{k} \tag{4}$$

$$P_k = \mu_T\left[\nabla U:(\nabla U + (\nabla U)^T) - \frac{2}{3}(\nabla.U)^2\right] - \frac{2}{3}\rho k\nabla.U \tag{5}$$

, and energy equation:

$$\rho C_p U.\nabla T = \nabla.(K\nabla T) + Q + Q_{vh} + W_p \tag{6}$$

$$\mu_T = \rho C_\mu \frac{k^2}{\epsilon} \tag{7}$$

Turbulence model parameters are (Naeeni, and Yaghoubi, 2007):

$C_{e1} = 1.44$ $C_{e2} = 1.92$ $C_{\mu} = 0.09$

$\sigma_k = 1$ $\sigma_e = 1.30$ $k_v = 0.41$

Hydrodynamic boundary conditions are analysis as:

- Inlet

Inlet velocity:

$$U_o = u \tag{8}$$

Turbulent intensity: (Rafah Aziz Najim, 2007)

$$l_T = \frac{0.16}{(Re_i)^{0.125}} \tag{9}$$

Turbulence length scale: (Rafah Aziz Najim, 2007)

$$L_T = 0.07 Dh_i \tag{10}$$

Where:

$Re_i = \frac{\rho u Dh_i}{\mu}$ Reynolds number at entrance.

$Dh_i = \frac{4(9W*\pi W)}{2(9W+\pi W)}$ Hydraulic diameter at entrance.

- Outlet

Outlet pressure: (Rafah Aziz Najim, 2007)

$$P_o = 0 \tag{11}$$

The above boundary condition is used widely in the literatures in order to ensure the flow from the boundary to the outside domain.

$$\left[-PI + (\mu + \mu_T)(\nabla U + (\nabla U)^T) - \frac{2}{3}(\mu + \mu_T)(\nabla . U)I - \frac{2}{3}\rho k I\right] n = -P_o^* n \tag{12}$$

$$P_o^* \leq P_o \tag{13}$$

$$\nabla k . n = 0 \tag{14}$$

$$\nabla \epsilon . n = 0 \tag{15}$$

- Walls

$$\left[(\mu + \mu_T)(\nabla U + (\nabla U)^T) - \frac{2}{3}(\mu + \mu_T)(\nabla . U)I - \frac{2}{3}\rho k I\right] n = -\rho \frac{U_\tau}{\delta_w^+} U_{tang} \tag{16}$$

$$U_{tang} = U - (U . n)n \tag{17}$$

$$\epsilon = \rho \frac{C_\mu k^2}{k_v \delta_w^+ \mu} \tag{18}$$

3. NUMERICAL MODEL

A full-scale Euro trough solar collector studied in the present work, where the specifications of the trough tabulated in Table 1. The absorber made from stainless steel with outer and inner diameters of 6.6 cm and 7 cm, respectively (Eckhard Lüpfert and etal, 2001).

The computational domain is defined by (5*W) in the upstream direction, (20*W) in the downstream direction, (9*W) in the cross direction and (π*W) in the span-wise direction, where W=5.8m is the aperture of the parabola as shown in Fig. 3.

The assumptions of the present work are: The fluid flow at the inlet assumed uniform. The uniform velocity assumption represents the worst-case for structural loading (Daniel, Premjit, et. al., 2011). The Prandtl number is set to Pr = ν/κ = 0.7 for air. The temperatures of the glass cover and ambient air are fixed at Trt = 350K and T_{amb} = 300K, respectively. A Neumann boundary condition ($\partial T/\partial n = 0$) is prescribed in the top, bottom and outlet boundaries for temperature.

The mesh refined around the collector surface; the HCE near wake and, stretched away from the collector. The mesh suited for each case of pitch angle and with respect to the dimension of the problem. In order to capture the flow structures near wake of the trough collector and around the HCE, mesh requirements are higher in these zones. However, due to the large difference between the dimensions of the aperture of the parabola and the receiver tube, the construction of the mesh is quite dense and complicated near these elements as shown in Figs. 4 and 5.In Table 2, the main characteristics of the meshes used for each pitch angle given.

The model treated as non-isothermal flow with turbulent k-ε model. The heat transfer done by forced convection for θ = 0º, and 90º, and by mixed free and forced convection for θ = 180º. The reason behind these assumptions is the value of airflow velocities near the heat transfer region.

The present problem solved by using a finite difference method using COMSOL Multiphysics v4.4 Program solver. The iterative solution considered to converge when the maximum of the residual across all nodes is less than 10^{-6} for continuity, velocities, and temperature.

The numerical results checked for grid independency. The procedure repeated when increasing the number of nodes until a stage reached where the results produce negligible changes with further refinement in grid size. The meshing refined near the trough collector, and it extra refined near the receiver due to big change in thermal and momentum values.

Validation of the resent work is obtained by the comparison of the thermal results of (Hachicha, A. A., et.al, 2012), where a good agreement is shown in Table 3.

Table 1. The specification of the Euro trough solar collector (Eckhard Lüpfert and etal, 2001)

Layout	parabolic trough collector
Support structure	steel frame work, pre-galvanized, two variants with light weight, low torsion
Collector length	12 m per element; 100 - 150 m collector length
Drive	hydraulic drive
Max. wind speed	operation: 14 m/s; stow: 40 m/s
Tracking control	Mathematical algorithm + angular encoder checked by sun sensor
Parabola	$y = x^2/4f$ with f = 1.71 m
Aperture width (W)	5.8 m
Reflector	28 glass facets per SCE
Absorber tube	evacuated glass envelope, UVAC® or other, application dependent
Fluid	oil, steam, application dependent
Cost	< 200 Euro/m^2

Table 2. Details of adopted meshes for each pitch angle

Pitch angle	0°	90°	180°
Number of element	90929	45765	31256
Minimum mesh quality	0.6376	0.6111	0.6475
Average mesh quality	0.9703	0.9724	0.97

Tabe 3. The validation datas.

	Position	Nua	Nu_{fsp}	Nu_{max}/Pos	Nu_{min}/Pos
Hachicha, A. A., et.al, 2012	0°	24.5	33.1	41.4/289.5°	9.5/196.8°
Present work	0°	25.8	32.79	34.38/313.7°	10.9/132.5°
Hachicha, A. A., et.al, 2012	90°	47.4	86	86/0°	27.3/222°
Present work	9°	48.3	67.7	69.8/22°	19.99/204.8°
Hachicha, A. A., et.al, 2012	180°	22.5	23.7	29.1/269.5°	7.4/85.9°
Present work	180°	21.66	19.1	25.82/188.8°	15.64/56.3°
Hachicha, A. A., et.al, 2012	Cylinder in cross flow	52.2	86	86.57/357.4°	17.4/272.2°
Present work	Cylinder in cross flow	47.4	45.37	45.37/360°	17.16/207.9°

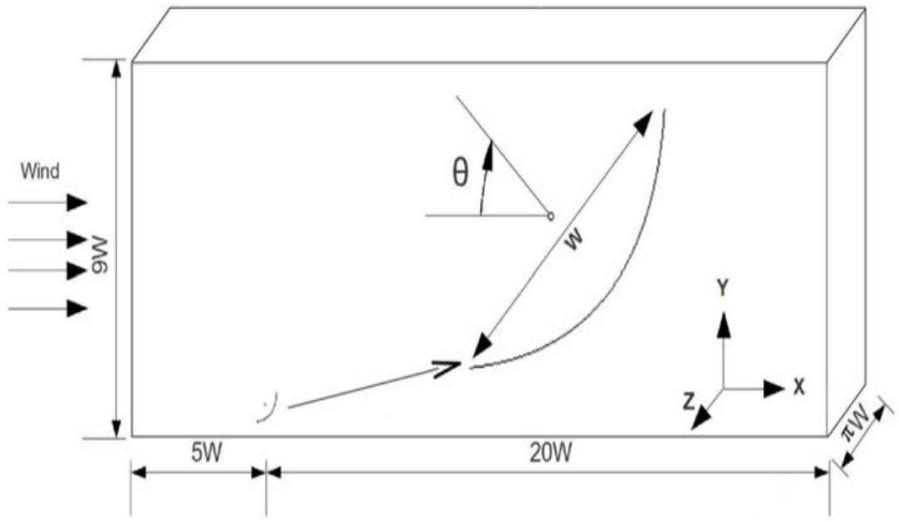

Fig. 3. Computational domain of the wind flow study around Euro trough solar collector (Daniel, Premjit, et. al., 2011)

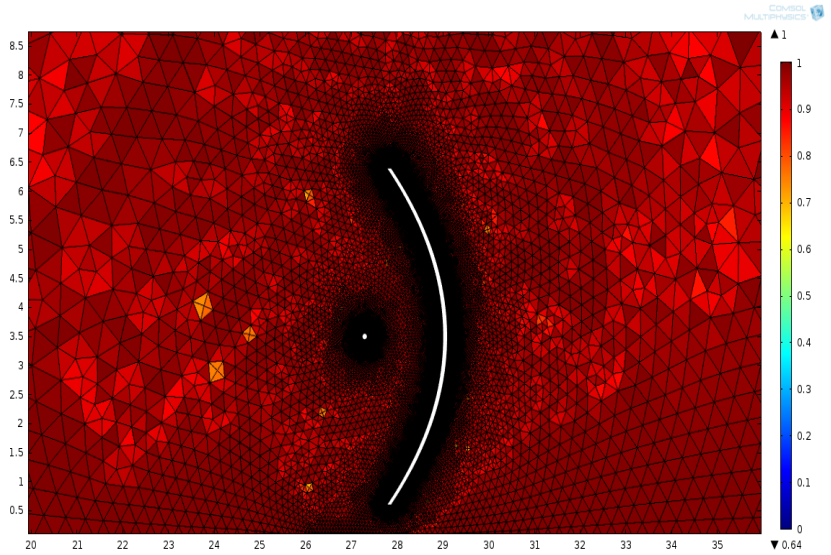

Fig. 4. Mesh Quality around the mirror and HCE

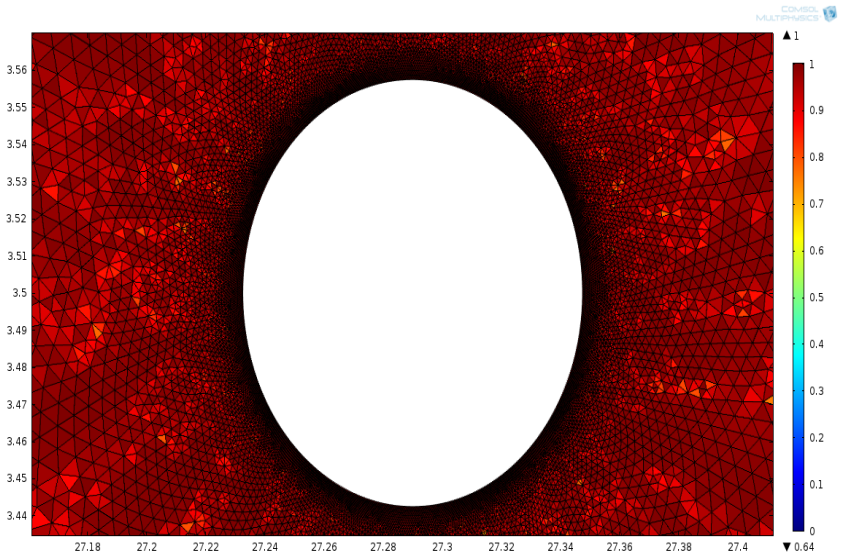

Fig. 5. Mesh quality around the HCE (Heat Concentration Element)

4. RESULTS AND DISCUSIONS

Since, the purpose of the present work is to reduce the heat lost from the receiver, and then it is important to demonstrate the side effect on the fluid flow. The results discussed focused on the area of trough and near the absorber. Three different orientations and velocity values taken. Figs.6 and 7 show the velocity vectors of air in the area of calculations. The behavior of airflow agreed with the literature (Naeeni, N, and Yaghoubi, M., 2007). Fig. 8 shows the streamlines and pressure contours on the collector with $\theta=0^o$, and focusing on the area near the absorber. The results show a constant air (v=0) around the absorber since it lies in the shadow of the plate added. This predict a reduction in heat transfer process since the convection should be free within these limits of airflow velocity. In Fig. 9 the streamlines and pressure contours are presented for $\theta=90^o$. It is noticed the low velocity of air near the absorber with the formation of eddies at the end of the half-circular plate at the downstream of the flow with smaller eddy at the upstream of the plate. Fig. 10 concerning with results of $\theta=180^o$. The streamlines show

a bundle of still air passing from the lower tip of the trough and rises gradually with the stream passing through the absorber. Figs.11 and 12 show the average pressure on the collector for various collector orientations and wind speed. It is obvious that the pressure is insensitive to the shape change, where the values of the angles 0^o and 180^o show no change in the pressure value with wind speed variation. In the other hand, at $90^o$the pressure shown to decrease with the increase in ratio between the plate diameter to the absorber diameter. This is a good advantage after all.

Fig. 13 shows the pressure coefficient on the collector with different radius ratios, collector orientations, and air velocities. At $\theta=0^o$, the increase in radius ratio causes the pressure coefficient to decrease (except for the case of dr=1.3). The same observations shown in $\theta=180^o$ (but the exception here shown at dr=2). The behavior shown to differ at $\theta=90^o$, where the increase in radius ratio causes the pressure coefficient to increase.

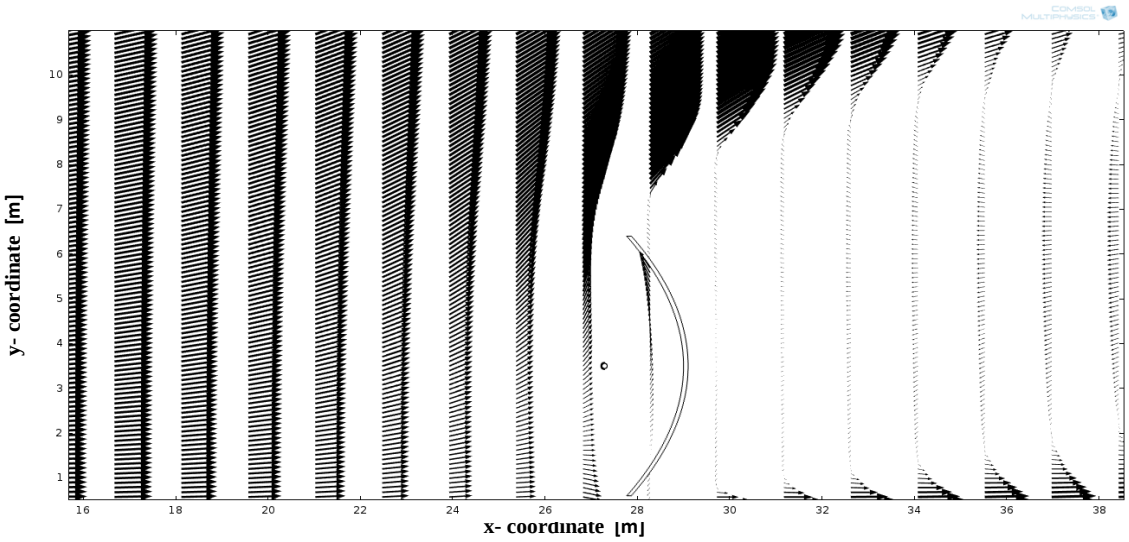

(a) θ=0º

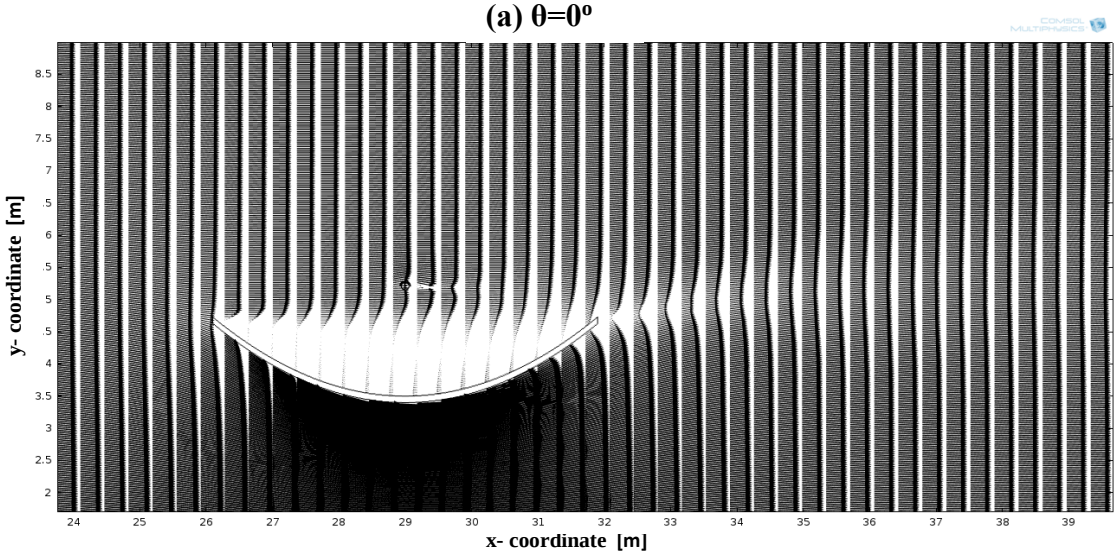

(b) θ=90º

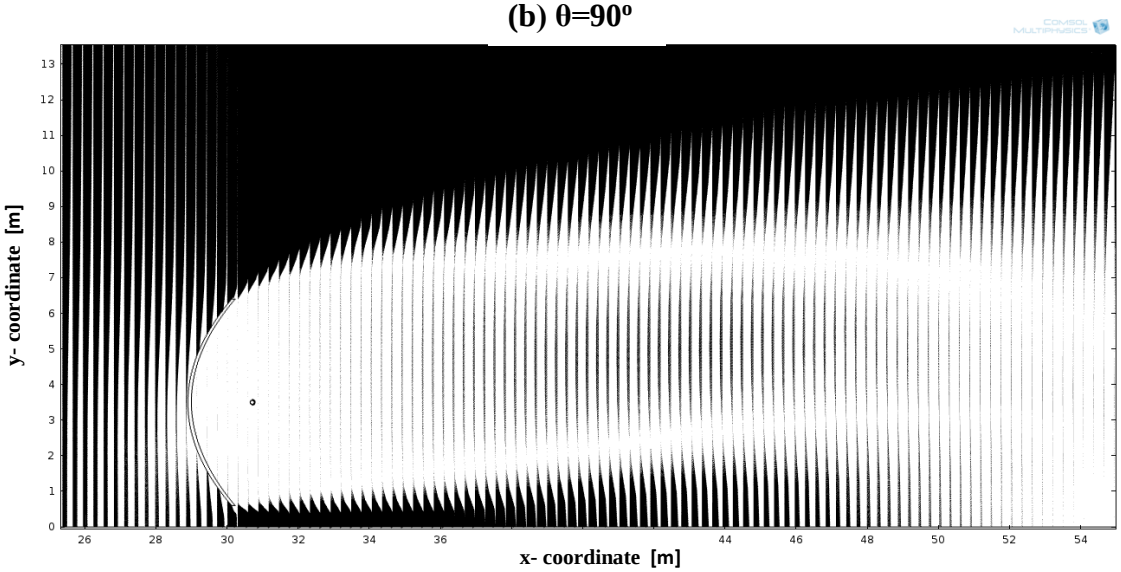

(C) θ=180º

Fig. 6. Velocity vectors for different pitch angles (U= 5 m/s, Dr=1.3): (a) θ=0º, (b) θ=90º, (c) θ=180º

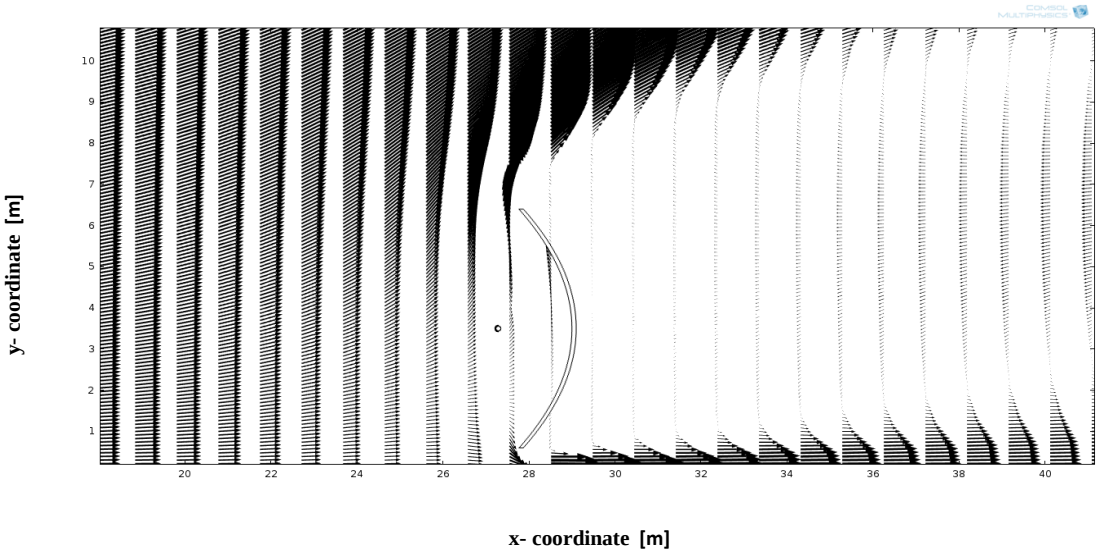

(a) θ=0º

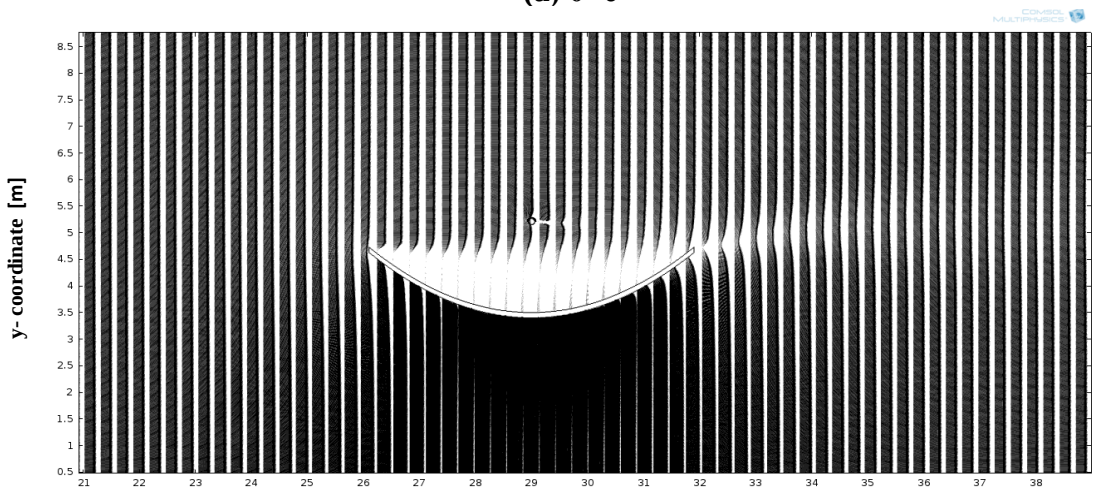

(b) θ=90º

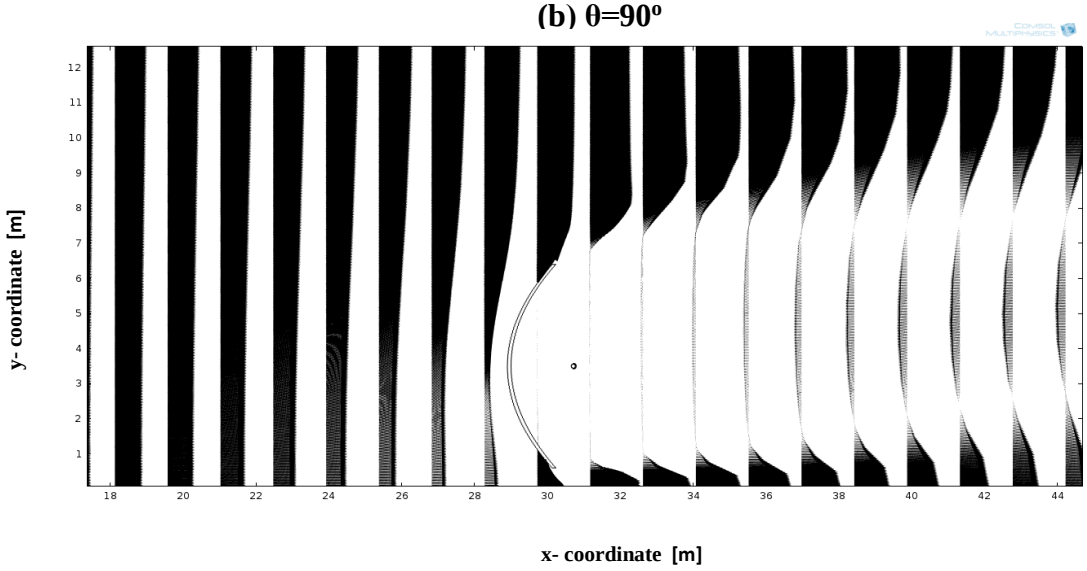

(C) θ=180º

Fig. 7. Velocity vectors for different pitch angles (U= 10 m/s, Dr=1.3): (a) θ=0º, (b) θ=90º, (c) θ=180º

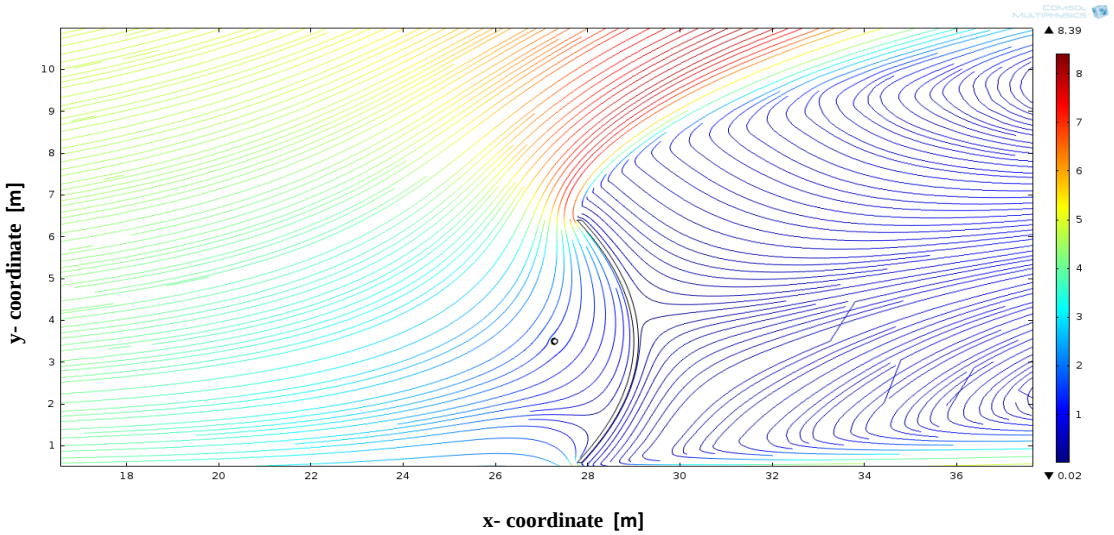

(a) stream lines with velocity filed (m/s)

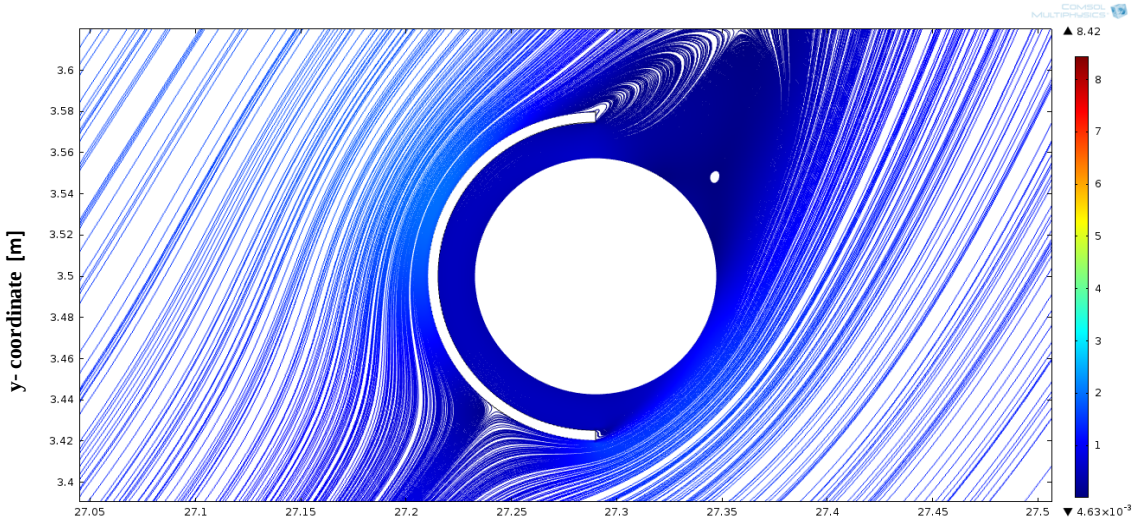

(b) stream lines near the collector with velocity filed (m/s)

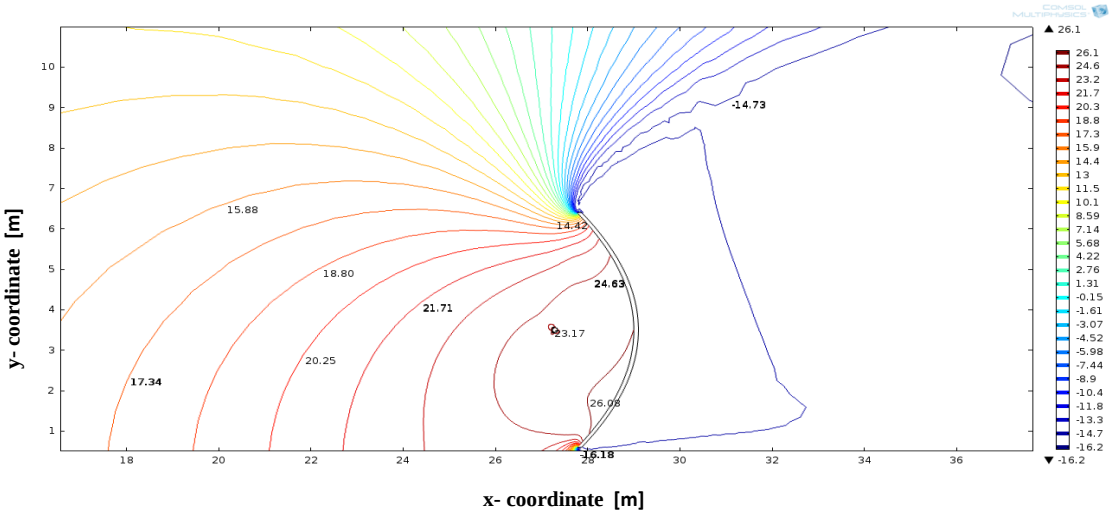

(c) pressure contours (Pa)

Fig. 8. Stream lines and pressure contours for collector at pitch angles θ=0º (U= 5 m/s): (a) stream lines; (b) stream lines near the collector and (c) pressure contours (Pa)

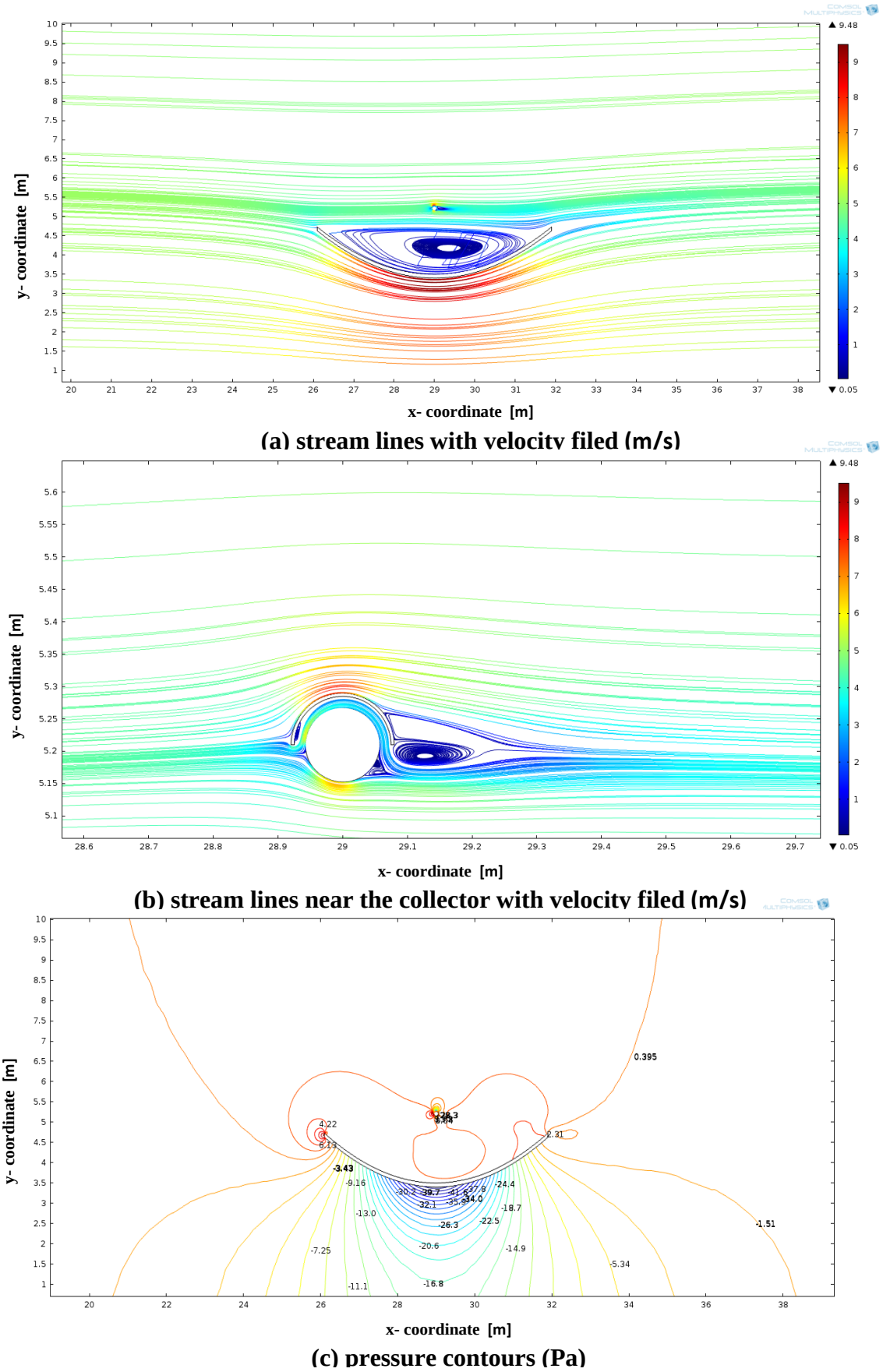

Fig. 9. Stream lines and pressure contours for collector at pitch angles θ=90º (U= 5 m/s): (a) stream lines; (b) stream lines near the collector and (c) pressure contours (Pa)

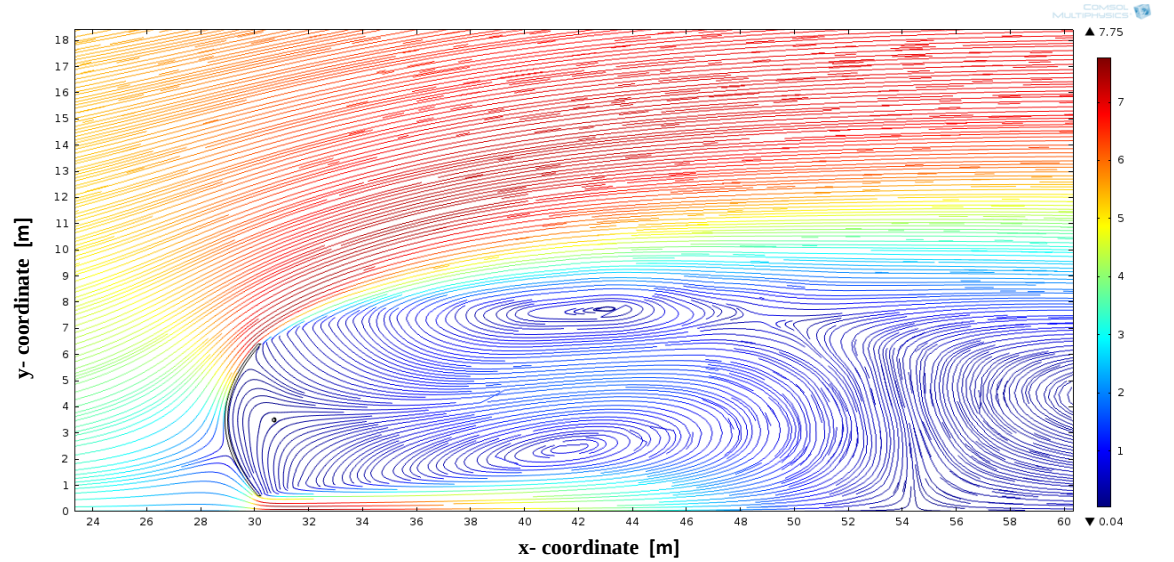

(a) stream lines with velocity filed (m/s)

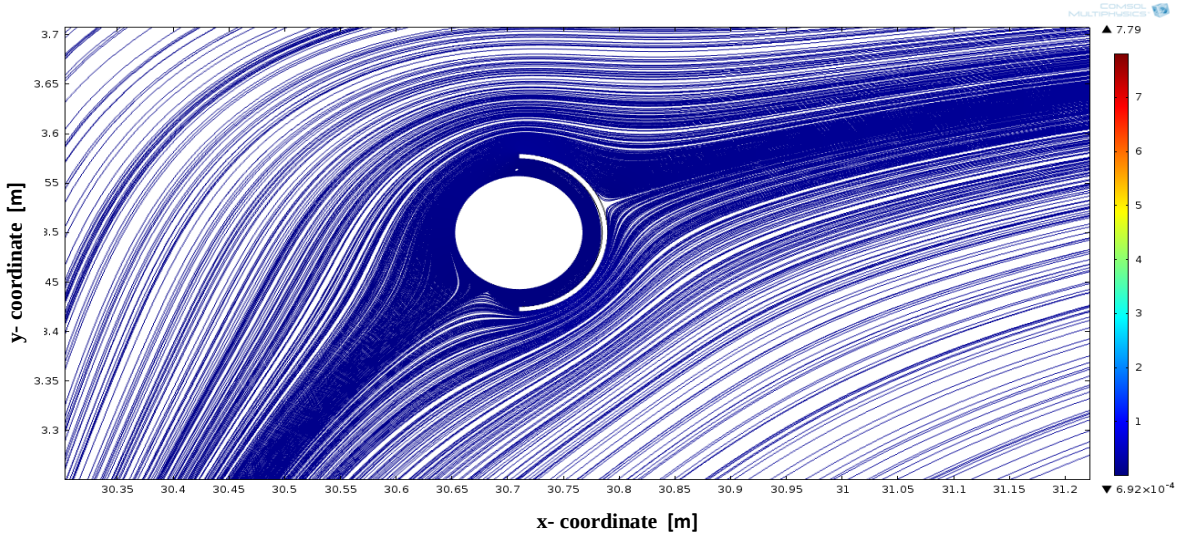

(b) stream lines near the collector with velocity filed (m/s)

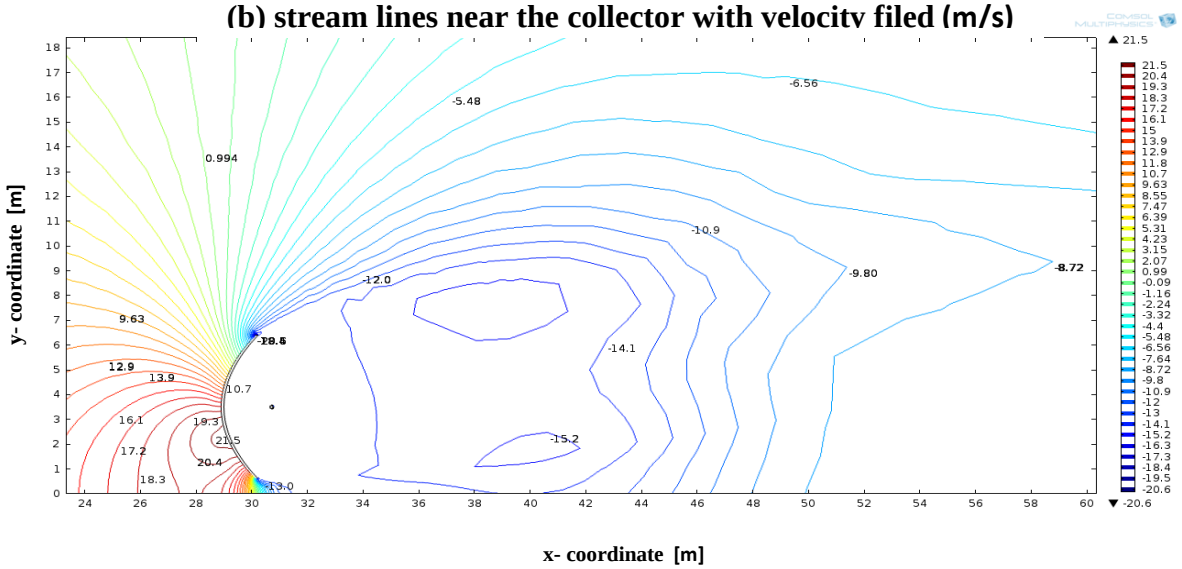

(c) pressure contours (Pa)

Fig. 10. Stream lines and pressure contours for collector at pitch angles θ=180º (U= 5 m/s): (a) stream lines; (b) stream lines near the collector and (c) pressure contours (Pa).

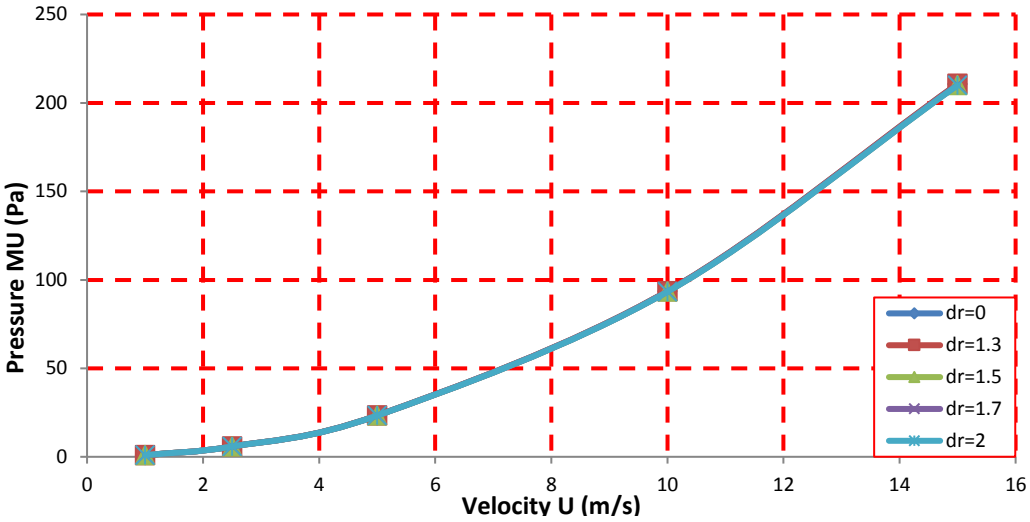

(a) θ=0°

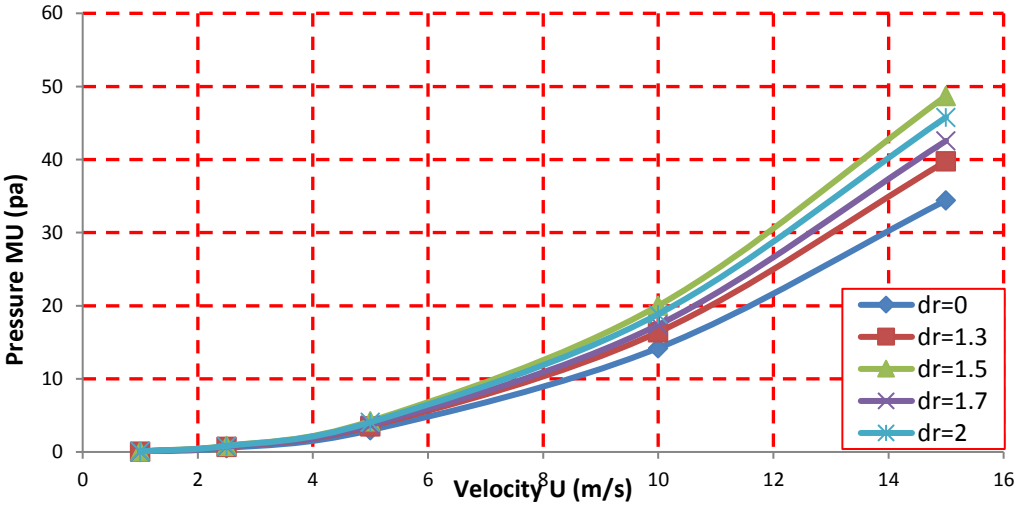

(b) θ=90°

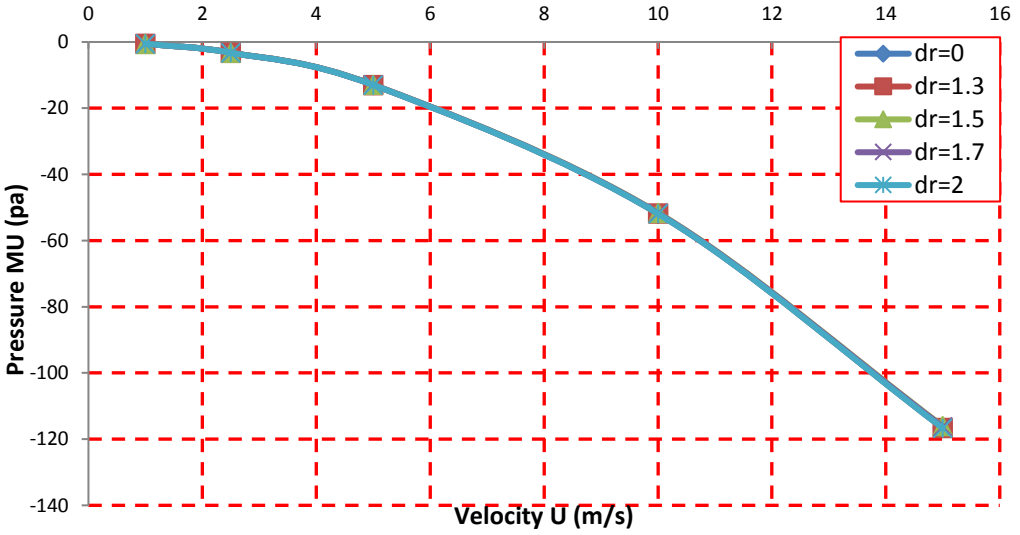

(c) θ=180°

Fig. 11. Variation of average pressure MU on the collector for various collector orientations and wind velocities: (a) θ=0°, (b) θ=90°, (c) θ=180°

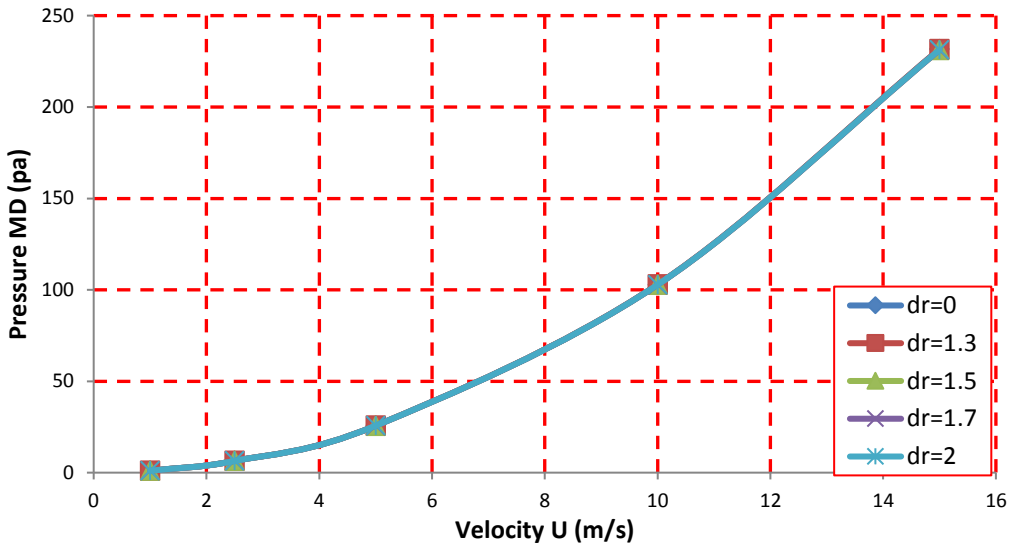

(a) θ=0º

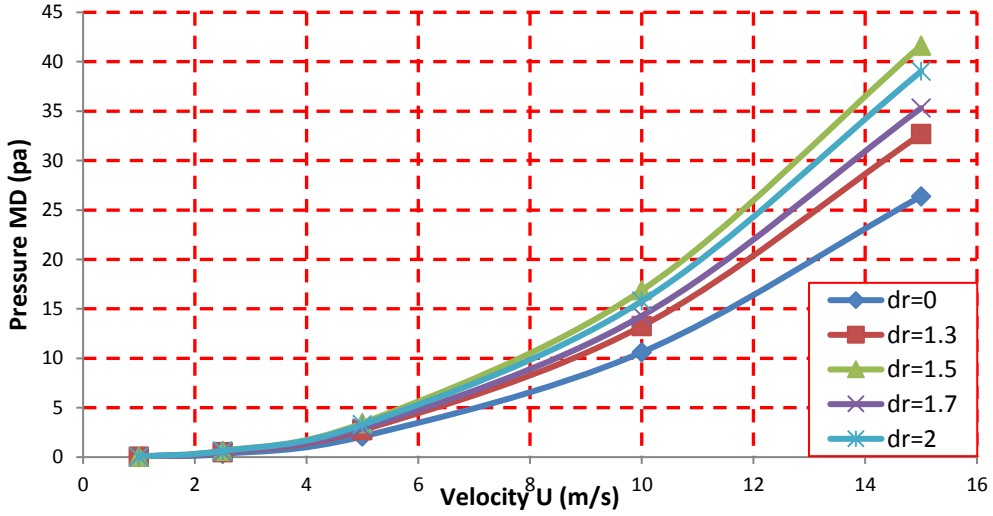

(b) θ=90º

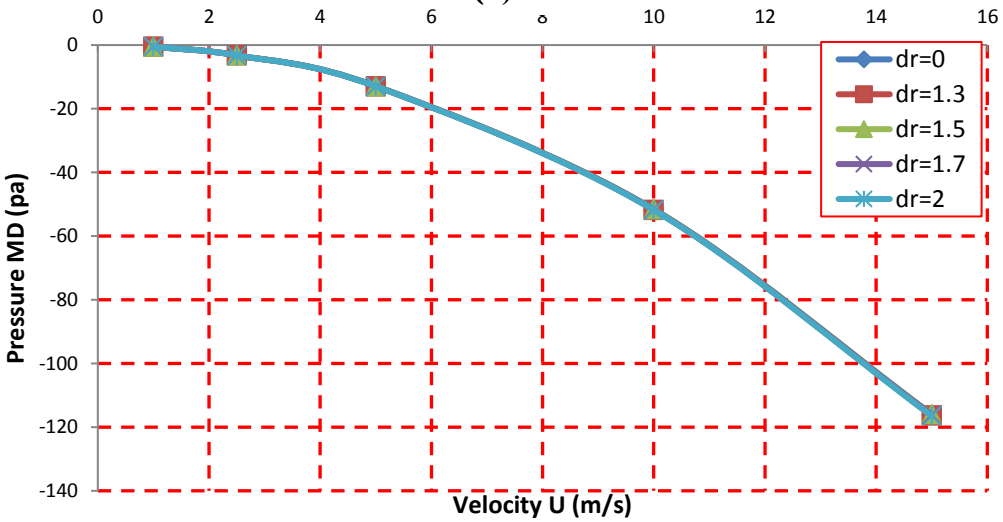

(c) θ=180º

Fig. 12. Variation of average pressure MD on the collector for various collector orientations and wind velocities: (a) θ=0º, (b) θ=90º, (c) θ=180º

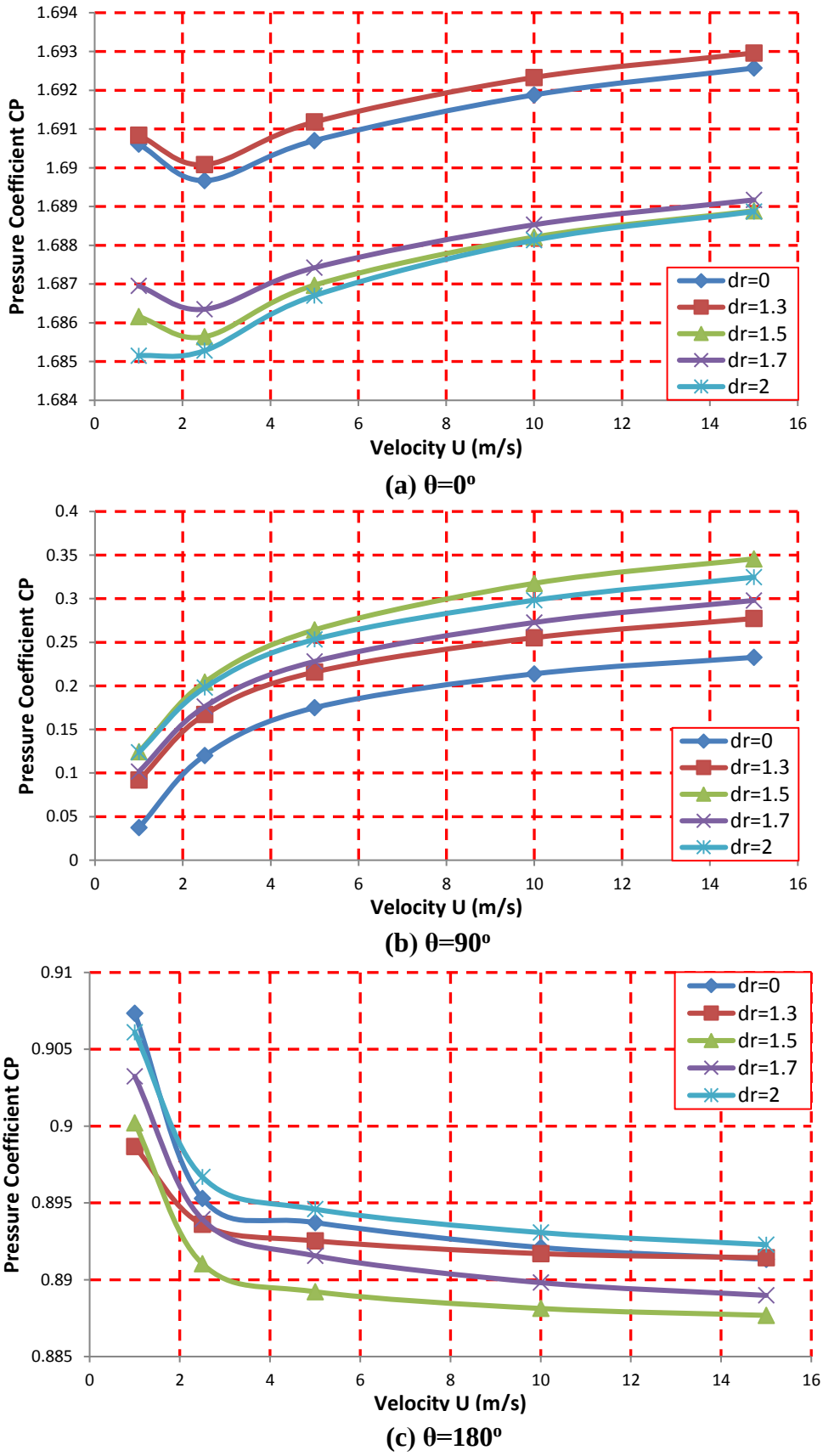

Fig. 13. Variation of pressure coefficient CP on the collector for various collector orientations and wind velocities: (a) θ=0°, (b) θ=90°, (c) θ=180°

5. CONCLUSIONS

The present work shows that the addition of a half-circular disc in front of the receiver surface may play an important role in heat transfer process, due to the dramatic change in the flow near it. The flow shown to be slow, or constant. This lead to change of heat transfer process to be transmit from forced convection to natural convection. The results show no side effect on the fluid flow such as, change in aerodynamic forces.

6. REFERENCES

Al-Ansary, Hany, and Zeitoun, O., 2011,"Numerical study of conduction and convection heat losses from a half-insulated air-filled annulus of the receiver of a parabolic trough collector", Solar Energy, pp. 3036-3045.

Cheng, Z. D., et.al.,2012 "Numerical simulation of a parabolic trough solar collector with nonuniform solar flux conditions by coupling FVM and MCRT method", Solar Energy, 86, pp. 1770-1784.

Christo, Farid C., 2012 "Numerical modelling of wind and dust patterns around a full-scale paraboloidal solar dish", Renewable Energy, 39, pp. 356-366.

Daniel, Premjit, et.al., 2011, "Numerical investigation of parabolic trough receiver performance with outer vacuum shell", Solar Energy, 85, pp. 1910-1914.

Eckhard Lüpfert, Michael, and et. al, 2001, "Euro trough Design Issues and Prototype Testing at Psa", Proceedings of Solar Forum 2001 April 21-25, 2001, Washington, DC, ASME.

Gong, Bo, et.al, 2012, "Field measurements of boundary layer wind characteristics and wind loads of parabolic trough solar collector", Solar Energy, 86, pp. 1880-1898.

Gu, Ming, 2009, "Study on wind loads and responses of tall buildings and structures", The Seventh Asia-Pasific Conference on Wind Engineering, November 8-12.

Hachicha, A. A., et.al, 2013, "Numerical simulation of wind flow around a parabolic trough solar collector", Applied Energy 107, pp. 426–437.

Kalogirou, Soteris, 2012, "A detailed thermal model of a parabolic trough collector receiver", Enrgy, 48, pp. 298-306.

Kazem, Aladine Abdulkader, and Hussein, Khalid Hameed,2013, "Study on the effect of the curvature of solar collector on wind loading coefficients and dynamic response of solar collector", Al-Khawarizmi Engineering Journal, vol. 9, No. 2, pp. 21-32.

Naeeni, N, and Yaghoubi, M., 2007, "Analysis of wind flow around a parabolic collector (1) fluid flow", Renewable Energy, 32, pp. 1898-1916.

Naeeni, N, and Yaghoubi, M., 2007, "Analysis of wind flow around a parabolic collector (2) heat transfer from receiver tube", Renewable Energy, 32, pp. 1259-1272.

Padilla, Ricardo Vasquez, et.al. 2011, "Heat transfer analysis of parabolic trough solar receiver", Applied Energy, 88, pp. 5097-5110.

Rafah Aziz Najim, "Numerical Prediction of a Solar Chimney Performance Using CFD Technique", PhD Thesis, Electromechanical Engineering Department / University of Technology, 2007.